ANALYSIS OF STRUCTURAL RESPONSE AND INSTRUMENTS

(SESSION II)

The questions not answered in a written form by the author do not appear on the pages of discussion.

NON-LINEAR RESPONSE ANALYZERS AND APPLICATION
TO EARTHQUAKE RESISTANT DESIGN

By RESPONSE ANALYZER COMMITTEE*

Introduction

According to the theory of vibration, it is estimated that during earthquakes ordinary structures will be subjected to much larger acceleration than are observed at the ground surface. These structures will be overstressed beyond the elastic limit in case of a severe earthquake if the structures are assumed to behave as an elastic body with small damping.

Since about 1930, it has been considered generally in Japan that actual building structures can resist severe earthquakes without destruction because of various damping sources; the main damping source not being the viscosity of the construction materials but the plastic deformation of the structures or foundations. To understand the characteristics of plastic deformation of structures, many Japanese investigators have studied the hysteresis characteristics of the load-deflection curve for various structural elements subjected to alternating load, (1) and (2). On the other hand, study into the dynamic nature of the problem did not develop for many years. However, a study was made to find the relationship between the energy absorption and amplitude decrement of the free vibration of structures with hysteresis characteristics, (3).

In 1953, the present Analyzer Committee constructed the type RAC-I linear response analyzer, (4). This is an electro-mechanical analog computer used to get the response of an elastic structure to an earthquake. In 1955, the type RAC-II response analyzer was made by TAKAHASI and AIDA to study the non-linear system with third order restoring force. For the purpose of studying the non-linear response of an elasto-plastic structure, the Committee later designed the type RAC-III non-linear response analyzer for a one-mass system, completing it in 1958. The type RAC-III is also a kind of electro-mechanical analog computer.

There have been several papers published in the United States and Japan, (5) (6) and (7), which investigate the non-linear response of elasto-plastic structures to earthquakes by means of either an electrical analog computer or a digital computer. The analyzer RAC-III characteristically deals with such special hystereses as shown in Fig. 2.

---

* Kiyoshi MUTO, Prof. Eng. Fac., Tokyo univ.; Ryutaro TAKAHASI, Prof. Earthq. Res. Inst., Tokyo Univ.; Isamu AIDA, Earthq. Res. Inst., Tokyo Univ.; Norihira ANDO, Prof. Eng. Fac., Yokohama Univ.; Toshihiko HISADA, Building Res., Inst.; Kyoji NAKAGAWA, Build. Res. Inst.; Hajime UMEMURA, Eng. Fac., Tokyo Univ.; Yutaka OSAWA, Eng., Fac., Tokyo Univ.

This paper describes mainly the mechanism of the type RAC-III non-linear analyzer and also illustrates the results obtained by the RAC-III of the non-linear response of a one-mass system to actual earthquakes. The El Centro California earthquake of 1940 has been used as one of the actual earthquakes applied to the type RAC-III. This was done so that the reader can compare the results with those obtained by other investigators and critically evaluate the method which is employed in this paper.

Linear Response Analyzer Type RAC-I

Although the purpose of this paper is to deal with non-linear response analyzers, the authors want to give, as first, some explanations about the type RAC-I linear response analyzer. It is believed that these explanations will make it more easy to understand the non-linear response analyzers, since they have been developed from the former.

The type RAC-I is an electro-mechanical analog computer in which a torsion resonator just like the galvanometer of an electromagnetic oscillograph is used to similate a one-mass system. The proper period of the resonator is 0.1 sec. The angular deflection of the resonator represents exactly the response to an earthquake of an elastic structure with the same period as the resonator if a current proportional to the earthquake acceleration $\alpha(t)$ is fed through the coil of the resonator.

In this case the equation of motion of the resonator can be written as

$$\frac{d^2\theta}{dt^2} + 2\varepsilon\frac{d\theta}{dt} + k^2\theta = G\alpha(t) \qquad \text{.....(1)}$$

If the current which flows through the driving coil is modulated n times as fast as the actual acceleration, the torque acting on the resonator becomes $G\alpha(nt)$, then Eq. (1) can be written as

$$\frac{d^2\theta}{d(nt)^2} + \frac{2\varepsilon}{n}\frac{d\theta}{d(nt)} + \frac{k^2}{n^2}\theta = G\frac{1}{n^2}\alpha(nt) \qquad \text{.....(2)}$$

Eq. (2) shows that, in the time-scale of nt , θ represents the displacement of a one-mass system which has the proper period $T=0.1\times n$ sec. and is subjected to an earthquake acceleration $1/n^2$ times the true value.

Accordingly, if the maximum deflection in each response is plotted against T , we get the "acceleration spectrum" as defined by Housner (8). To get the "velocity spectrum", it is necessary to multiply each ordinate by its corresponding value of T . The fraction of the critical damping $h=\varepsilon/k=\varepsilon/n \div k/n$ of the resonator remains constant even if we change the time scale. This is the merit of this method compared with the alternative method of changing the period of the resonator (9).

The arrangement of the type RAC-I analyzer is shown schematically in Fig. 1. It consists of three parts: the torsion resonator, an amplifier set and a part consisting of recording drum, photo-tube head, two motors and two tachometers, etc. The resonator, having a period of 0.1 sec., is a sort of galvanometer with three coils. These coils are imbedded in a bar of metacrylic resin, 3 mm in diameter and 125 mm long, which is spanned by two pieces of phospor bronze ribbon between pole pieces of magnets. Two of the coils are fed with the driving current. From the third coil a voltage increment is taken out to be fed back to the amplifier. By adjusting the amount and sense of the feed-back voltage, we can fix the damping of the resonator at any value between zero and the critical. The driving current is modulated by means of the photo-tube head (PT25V x 2), the amplifier and a black and white film of the accelerogram to be analyzed. The driving current flows through the two coils in such directions as to cancel in each other the effect of the plate D. C.

A mirror is provided to the resonator to record its angular deflection on a sheet of photographic paper wound on the recording drum. This drum has a common axis with the accelerogram film drum.

In order that the resonator, 0.1 sec. in proper period, shall represent buildings of periods of from 0.1-5.0 sec., the accelerogram film drum has to be rotated at the speed 1 - 50 r.p.m., if the total length of the accelerogram film corresponds to the earthquake motions during 1 min. To vary the rotation speed in this wide range, we have used a combination of a differential gear, a synchronous motor and a D. C. motor as shown in Fig. 1. An automatic control device consisting of a servo-amplifier, a voltage stabilizer and two tachometers is provided to the D. C. motor to maintain its speed at any preset value.

The automatic switches next to the recording drum control a shutter to open only for the interval of one revolution of the recording drum, although the drum is making many revolutions. The switches also make the damping of the resonator critical during the final 1/6 part of each revolution. This is to have the resonator start from the undisturbed state in each revolution.

In this way, we can get response curves of buildings of different periods, traced side by side on a sheet of photographic paper. This is another point of merit for this type of response analyzer.

For further details of the type RAC-I analyzer, readers are referred to report (4) in the bibliography.

Non-linear Response Analyzer, type RAC-III, for One-mass System with a Hysteretic Bi-linear Restoring Force

Before entering into the description of the type RAC-III non-linear response analyzer, we will give a short description of the type RAC-II non-linear response analyzer. This analyzer is for use with a one-mass system with a non-linear restoring force but with no hysteretic characteristic. In this case, the force displacement characteristic describes a curve defined by an expression involving terms of third order or higher, but with no hysteresis loop. The restoring force in the type RAC-II analyzer is obtained in the following way:

A torsion resonator, similar to that used in the type RAC-I, has four coils. Two of them are for the driving current which is proportional to the earthquake acceleration. The third coil is used to control the damping of the resonator. The fourth coil is the restoring force coil through which a current proportional to $R(\theta)-k^2\theta$ is made to flow. In this expression θ is the angular deflection of the resonator, k^2 the restoring coefficient of the suspension wire and $R(\theta)$ is the desired restoring force. The current is obtained by amplifying the photoelectric currents from two photo-tubes which act in a push-pull way.

The image of a rectangular light source is produced on a screen by a mirror attached to the resonator. The screen has two windows. They are set apart from each other by the length of the rectangular image, and are symmetrically shaped with respect to the neutral position of the light image. The right window has a width proportional to $\frac{d}{d\theta}R(\theta)-k^2$, so that the quantity of light which enters the right window is proportional to $R(\theta)-k^2\theta$ when $\theta>0$. When $\theta<0$, that is when the light image is moved to the left, the left window acts in a similar way. There are two photo-tubes, one behind each window, and the outputs from these photo-tubes are fed to the amplifier in a push-pull way, as mentioned above. The type RAC-II analyzer has been applied to the study of motion of a ship under seaway.

We will now describe the type RAC-III non-linear response analyzer, which is the analog for a one-mass system with hysteretic, bi-linear restoring force.

As shown in the Appendix, the large amplitude vibration of some structures can be represented by the bi-linear hysteretic restoring characteristic as shown in Fig. 2. The point Q, which represents the state of vibration of the structure in the force-displacement plane, starts from the undisturbed position at point O and follows the straight line OP until it reaches the yield line AB at P. The displacement up to the point P is purely elastic. We will call this displacement δ_Y the maximum elastic displacement. The point Q then moves along the yield line as long as the velocity keeps the same sign. The displacement then consists of the maximum elastic displacement δ_Y and a yield displacement. When the displacement begins to decrease, the point Q follows the line RST which is parallel to OP, then the other yield line $A'B'$, and so on. When the external force completely disappears, there remains a permanent set such as OZ. The energy consumed in the structure is proportional to the shaded area in Fig. 2, or roughly proportional to the sum of the yield excursions such as RT, TU, and etc. We will call the value f_0, or the force corresponding to the yield point P, the yield-point force.

To realize this bi-linear restoring force in a torsion resonator similar to those used in the type RAC-I and the type RAC-II analyzer, a sliding mirror device as shown in Fig. 3 has been used. Referring to this Figure, C_1 is the driving force coil through which an electric current proportional to the ground acceleration is made to flow. C_2 is a coil for providing the resonator with the desired degree of damping by shunting the coil with an external resistance. Coils C_1 and C_2 are wound on the same frame. C_3 is the coil for providing the restoring force which is proportional to the rotation angle θ_M of the sliding mirror M. The coils are bound rigidly to each other by a connecting rod on which another mirror m is attached to record the deflection of the coils. The whole system is suspended by two wires W in the gaps between two magnets as shown in the Figure.

The sliding mirror M , which is at the top of the coil system, is fixed to an arm L which is fitted to the axis P of the moving coil system and rests on the friction seat F . The arm L extends through an adjustable gap between two stoppers G and G'. Thus the rotation angle θ_M of the mirror is restricted within the range $|\theta_M| \leqq \theta_e$, $2\theta_e$ being the angle subtended by the stoppers. If the rotation angle θ of the coils is in the range $|\theta| < \theta_e$, θ_M is equal to θ . If θ becomes equal to or greater than θ_e, the mirror arm L comes to contact with one of the stoppers G and the mirror begins to slide and remains at the position $\theta_M = \theta_e$ as long as $d\theta/dt$ keeps the same sign. As soon as θ begins to decrease, the mirror begins to rotate together with the coils until θ_M becomes $-\theta_e$. After that, the sliding mirror remains at the position $\theta_M = -\theta_e$ for the interval $d\theta/dt \leqq 0$.

If a photoelectric current is made proportional to the rotation angle θ_M , in a similar manner as in the type RAC-II analyzer, amplified, and fed to the coil C_2 , we can get the restoring torque which is proportional to θ_M . Beside this restoring torque, there is a feable torque due to the suspension wires which is obviously proportional to the rotation angle θ of the coils. We have, therefore, a partially plastic bi-linear restoring torque as shown in Fig. 2. The ratio γ^2 of the plastic restoring coefficient to the elastic one can be changed by varying the amplification of the photoelectric signals. ϕ_0 is the yielding point torque.

Now consider a one-mass system having partially plastic bi-linear restitutive character, subjected to the earthquake acceleration $\alpha(t)$. Let m be the mass, and $f(y)$ the restoring force. Then the equation of motion is

$$m\frac{d^2y}{dt^2} + 2\mu\frac{dy}{dt} + f(y) = -m\,\alpha(t)$$

Referring to Fig. 2, the yield-point force f_0 is

$$f_0 = f(\delta_Y) = K_Y \cdot g \cdot m$$

where K_Y is the fraction of gravity at the yield point of the structure and δ_Y the maximum elastic displacement. If we denote by T the proper period of the structure for elastic vibrations, we have the relationship

$$\frac{4\pi^2}{T^2} = \frac{f_0}{m\,\delta_Y} = \frac{K_Y \cdot g}{\delta_Y}$$

If the displacement and force are then expressed in terms of δ_Y and f_0 respectively, the equation of motion can be written as follows:

$$\frac{d^2\eta}{dt^2} + 2\varepsilon\frac{d\eta}{dt} + \frac{4\pi^2}{T^2}\chi(\eta, \gamma^2) = -\frac{4\pi^2}{T^2}\frac{\alpha(t)}{K_Y \cdot g} \qquad \ldots\ldots(3\text{-}1)$$

where $\eta = y/\delta_Y$, $\chi(\eta, \gamma^2) = f(y)/f_0$, and $\varepsilon = \mu/m$
The functional form of $\chi(\eta, \gamma^2)$ depends only on γ^2 , the ratio of the plastic restitutive coefficient to the elastic one, as can be seen from Fig. 2.

If the restitutive characteristic of the analog resonator is adjusted to have the form $\chi(\eta, \gamma^2)$, and the external driving torque is expressed as shown on the righthand side of the Eq. 3-2, then the motion of the analog resonator can be represented by

$$J\frac{d^2\theta}{dt^2} + 2\mu'\frac{d\theta}{dt} + \phi(\theta) = -\phi_0\frac{a(\frac{T}{T_0}t)}{K_Y \cdot g} \quad \ldots\ldots(3\text{-}2)$$

In terms of θ_e and $\phi_0 = \phi(\theta_e)$, which corresponds respectively to δ_Y and f_0 of the one-mass system under consideration, Eq. (3-2) becomes

$$\frac{d^2(\theta/\theta_e)}{dt^2} + 2\varepsilon\frac{d(\theta/\theta_e)}{dt} + \frac{1}{J\theta_e}\phi(\theta) = -\frac{\phi_0}{J\theta_e}\frac{a(\frac{T}{T_0}t)}{K_Y \cdot g}$$

or, since $\phi(\theta) = \phi_0\,\chi(\theta/\theta_e\ ,\ \gamma^2)$ and $\phi_0/J\theta_e = 4\pi^2/T_0$, T_0 being the proper period of the resonator,

$$\frac{d^2(\theta/\theta_e)}{dt^2} + 2\varepsilon\frac{d(\theta/\theta_e)}{dt} + \frac{4\pi^2}{T_0^2}\chi(\frac{\theta}{\theta_e}, \gamma^2) = -\frac{4\pi^2}{T_0^2}\frac{a(\frac{T}{T_0}t)}{K_Y \cdot g}$$

By changing the unit of time from t to $t' = \frac{T}{T_0}t$,

$$\frac{d^2(\theta/\theta_e)}{dt'^2} + 2\varepsilon\frac{d(\theta/\theta_e)}{dt'} + \frac{4\pi^2}{T^2}\chi(\frac{\theta}{\theta_e}, \gamma^2) = -\frac{4\pi^2}{T^2}\frac{a(t')}{K_Y \cdot g} \quad \ldots\ldots(3\text{-}3).$$

Comparing Eq. (3-3) with Eq. (3-1) will show that they are of the same form. This shows that if the accelerogram film is driven with the speed proportional to T/T_0 , then θ/θ_e, expressed in the same time scale, gives y/δ_Y of the actual structure. Thus the non-linear response of a structure with any proper period can be obtained.

In Fig. 4 the block diagram shows the general arrangement of the type RAC-III analyzer. In the Figure, PT_e and PT_r indicate photo-tubes and A_e and A_r the amplifiers. Suffixes e and r , respectively, mean earthquake and restoring forces. D is the resistor for damping, $R.D.$ the recording drum and $F.D.$ the film drum. Photos 2 and 3 show, respectively, the photo-tube box and the resonator of the type RAC-III analyzer.

Calibration and Testing of the type RAC-III analyzer

The actual restoring characteristic of the resonator mentioned above has been found to be as shown in Fig. 5. This figure was obtained by plotting the deflections of the resonator when a $D.C.$ current was fed through the driving coil. The ratio of the slope of the plastic portion to that of the elastic portion is $\gamma^2 = 1/9.2$ and the maximum elastic displacement is 12.5 mm on the recording paper.

The proper period of oscillation within the elastic range was found to be 0.11 sec. from the small amplitude oscillation of the resonator.

Dynamic testings of the resonator have been made to ascertain the behavior of the sliding mirror. The equation of motion of the resonator, excited by a stationary harmonic force $P \sin pt$, can be transformed into the following form

$$\frac{d\dot{\eta}}{d\eta} = \frac{-\dot{\eta}}{\eta + \delta} \quad , \qquad \delta = \frac{\chi(\eta, \dot{\eta}^2)}{\lambda^2} - \eta + \frac{2h}{\lambda}\dot{\eta} - \frac{P}{f_0 \lambda^2} \sin\tau \quad ,$$

where $\lambda = T_0/(2\pi/p)$ and the time scale is taken to be $\tau = pt$. Since this equation contains both the hysteretic characteristic and the damping proportional to the velocity $\dot{\eta}$, it is cumbersome to solve the equation analytically. The stationary amplitude can easily be estimated, however, by applying the phase-plane-delta method (10) to the initial two or three exciting force cycles. The fraction of critical damping is $h=0.07$.

Fig. 6 shows the comparison between the calculated results and the experimental results obtained on the recording photographic paper when a stationary harmonic accelerogram was applied to the present type RAC-III analyzer. The results of the experiment concide very well with the calculated results.

Non-linear Response as Obtained by type RAC Analyzers

An example of the response of the type RAC-III analyzer to a real earthquake accelerogram is shown in the upper part of Fig. 7. The accelerogram is that of the E-W component of the El Centro California earthquake which occurred on Dec. 30, 1934. The result corresponds to that of a structure with a period of 0.42 sec. The yield point acceleration $K_Y \cdot g$ of the structure is prefixed at 0.12g in this case.

In the lower part of the same Figure, we have shown how the point Q, designated in Fig. 2, has moved in the force-displacement plane. Each maximum or minimum of the response curve and the corresponding positions of the point Q have been shown by the same numerals. The graphs show how the point Q describes hysteresis loops and how the permanent set is developed in the structure. We shall remark here that the point Q comes to rest on the horizontal axis when the earthquake is finished. The distance between the final position of the point Q and the origin O corresponds to the final permanent set.

We have next analyzed several strong motion earthquakes as listed below and plotted their maximum over-all displacements against the proper period of a building. We will call this graph the spectrum of the over-all maximum displacement. The earthquake accelerograms used were from the following:

El Centro California Earthquake of Dec. 30, 1934,
E-W component;

El Centro California Earthquake of May 18, 1940,
N-S component;
Earthquake of Feb. 14, 1956, observed at Hongo, Tokyo, Japan,
N-S component;
Earthquake of Sept. 30, 1956, observed at Nihonbashi,
Tokyo, Japan, N-S component.

The accelerograms for the first and second earthquakes listed above were taken from the publication of CIT (8). Accelerograms of the third and fourth earthquakes were placed at our disposal through the courtesy of the Strong Earthquake Observation Committee of Japan. For each earthquake, the maximum over-all displacement was sought for 8 to 11 different building periods and for 2 to 3 different values of K_Y. Results are shown in Figs. 8 to 11.

The response of the analyzer is recorded on the photographic paper in the unit of δ_Y. The actual displacement of the building can be obtained easily if we calculate the actual value of δ_Y from the period of the building and the fraction of gravity K_Y corresponding to the yield point. The maximum over-all displacements plotted in Figs. 8 to 11 were obtained in this way in cm.

Suggestions for Future Aseismic Design

The results obtained to this date are too few to be used as a basis upon which to draw concrete conclusions for future aseismic design. We can, however, make some observations and suggestions of note as follows:

1. Comparing the maximum over-all displacement spectrum of the non-linear system with that of the linear system, it is to be noticed that the resulting difference between them is not as large as obtained previously by New Zealand Engineers (6). See Fig. 12 for this feature.

2. Inspection of test results seem to indicate that the maximum over-all displacement depends rather more upon the period of the building than on K_Y. This fact may suggest employment of a structural design method based upon the maximum displacement.

3. In the Appendix some of the load-distortion curves with hysteresis loops collected by the authors are presented. The parallelogram characteristic employed in this paper is a typical one which may represent the characteristics for reinforced concrete or steel structures, as can be seen in some of the Figures. It should be noticed, however, that the characteristics of other types of structures may be rather different from those used in this paper.

With respect to the displacement under consideration, attention should be paid to the nature of the displacement as it is related to structural types. In the case of open framed structures of either steel or reinforced concrete and without shear walls, the displacement is caused mainly by frame deformation and distortion. In the case of a more rigid structure such as a box-system frame of reinforced concrete or masonry, the displacement is a result mainly of the soil deformation under the fundations.

4. The significance of this type of a design approach is that it would enable an evaluation of the plastic deformation to be expected of a building structure during strong motion earthquakes. In Japan the standard seismic coefficient value is taken as 0.2 for conventional seismic design. Using this coefficient value, no severe damage to the structure is expected from a strong earthquake; however, it is suposed that the structural skeletion or foundation may undergo some plastic deformation. This plastic deformation can take the form of localized column hinge, diagonal cracks in seismic wall, etc.

Using the studies reported in this paper, we have quantitatively evaluated these plastic deformations to some extent. For example, consider the design of a structure which has $K_Y = 0.29$, $h = 0.07$ and a natural period of 0.4 seconds in the elastic range. From Fig. 9, this structure is expected to show a maximum deflection of about 5.5 cm. in case of an earthquake similar to that of the El Centro California Earthquake of May 18, 1940. It depends upon the design principle of the building under consideration as to which part this plastic deformation will affect. The results shown in the Appendix are fundamental data for such design. The deflection value mentioned herein will change for other earthquakes but such values can be predicted quantitatively within a certain range.

5. The value of the permanent set caused by earthquakes should be decided in accordance with accepted engineering practices. In the case of the structure used as an example in 4 above, the permanent set obtained is about one-third the maximum over-all displacements concerned, as can be observed in Fig. 13. This value of the permanent set might be considered as a criterion when elasto-plastic design is used.

Bibliography

(1) T. Taniguchi: "A Study on the Decrement of Vibration of Reinforced Concrete Member", Report of the Tokyo Institute of Technology, Vol. 10, 1934.

(2) R. Tanabashi: "Tests to Determine the Behaviour of Riveted Joints of Steel Structures under Alternate Bending Moments", Report of the Faculty of Eng., University of Kyoto, Vol. 8, No. 4, 1935.

(3) R. Sano and K. Muto: "Earthquake and Wind-proof construction" p. 156, Tokiwashobo, Tokyo, Japan, 1935.

(4) R. Takahasi: "A Response Computer Preliminary Report", Proceedings of the 3rd Japan National Congress for Applied Mechanics.

(5) Glen V. Berg: "The Analysis of Structural Response to Earthquake Forces", Industry Program of the College of Engineering, University of Michigan May, 1958.

(6) G. N. Bycroft, M. J. Murphy and K. J. Brown: "Electrical Analog for Earthquake Yield Spectra", Journal of the Eng. Mech. Div., Proc. of the ASCE, October, 1959.

(7) T. Kobori, K. Kaneta, R. Minai and K. Mizuhata: "Analog Computer Analyses of Nonlinear Transient Vibration of Structures", Transactions of Architectural Institute of Japan, October, 1959.

(8) Alford J. L., Housner G. W. and Martel R. R., (1951). "Spectrum Analyses of Strong Motion Earthquakes" First Tech. Rep. N6Onr - 24425.

(9) Biot M. A., (1941). Bull. Seism. Soc. Amer. Vol. 31., pp. 151-171.

(10) Jacobsen, L. S., and Ayre, R. S. "Engineering Vibrations", McGraw-Hill, 1958.

<u>Nomenclature</u>

$\alpha(t)$	= the ground acceleration
θ	= deflection angle of the resonator
t	= time
ε	= coefficient of damping
k^2	= restoring coefficient
G	= galvanometer coefficient
h	= fraction of critical damping
T	= proper period of the structure
T_0	= proper period of the resonator
$R(\theta)$	= restoring force of the resonator
δ_Y	= maximum elastic displacement
f_0	= yield-point force
θ_M	= rotation angle of the sliding mirror
θ_e	= angular deflection of the resonator corresponding to δ_Y
r^2	= ratio of plastic restoring coefficient to elastic one

ϕ_o	= yield-point torque
m	= mass of the one-mass system
$f(y)$	= restoring force of the one-mass system
μ, μ	= damping coefficient
K_Y	= fraction of gravity at the yield point
y	= displacement (linear) of the system relative to the ground
J	= moment of inertia of the resonator
η	= y/δ_Y

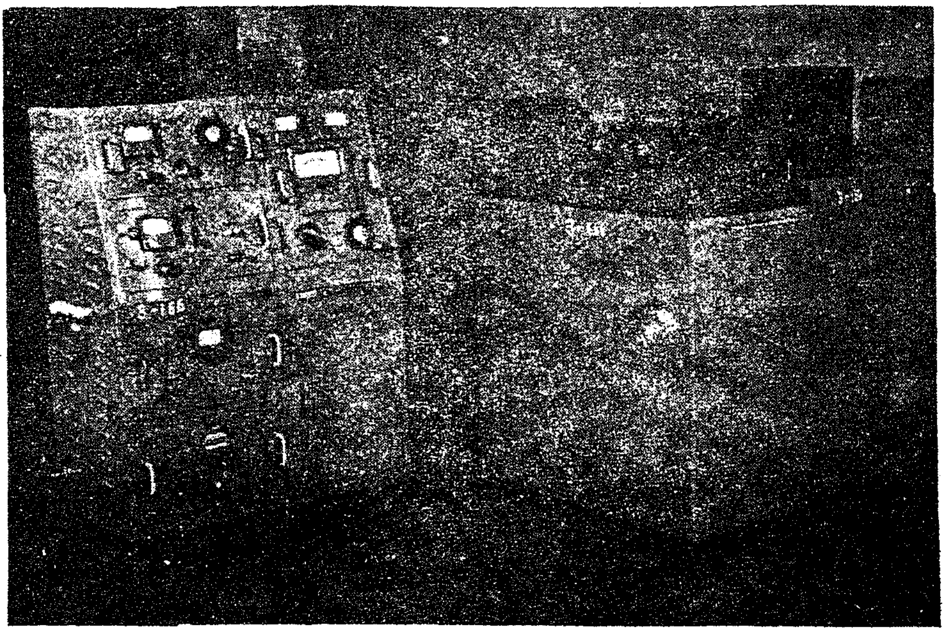

Photo. 1 Type RAC-I analyzer.

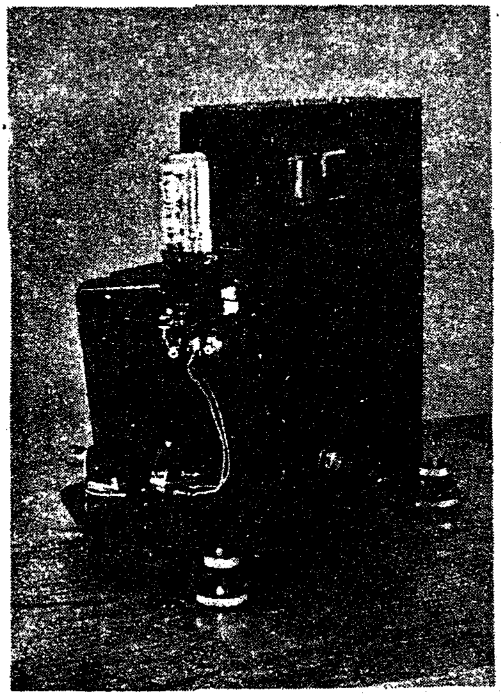

Photo. 2
Photo-tube box of the type RAC-III analyzer.

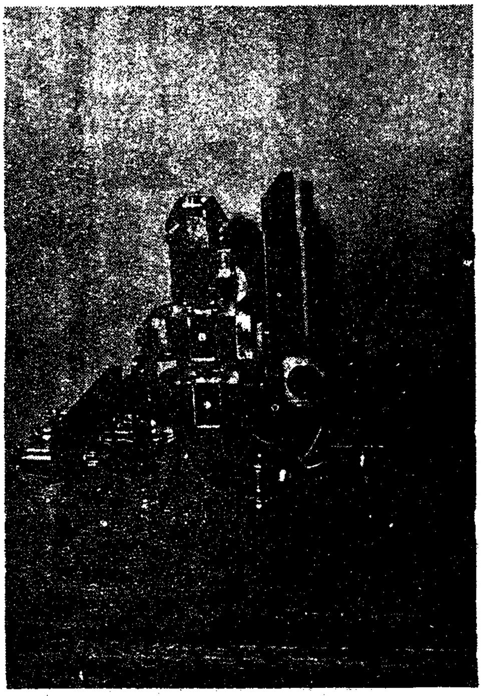

Photo. 3 Vibrator of the type RAC-III analyzer.

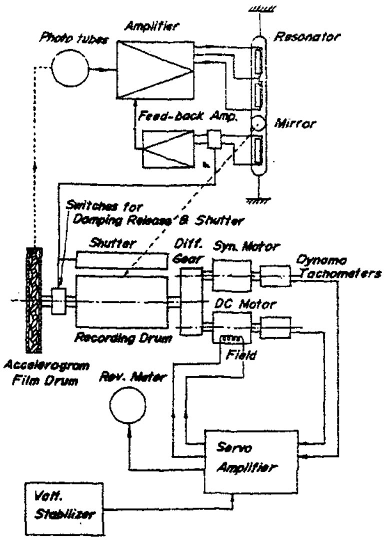

Fig. 1 Block diagram showing the general arrangement of the type RAC-I analyzer.

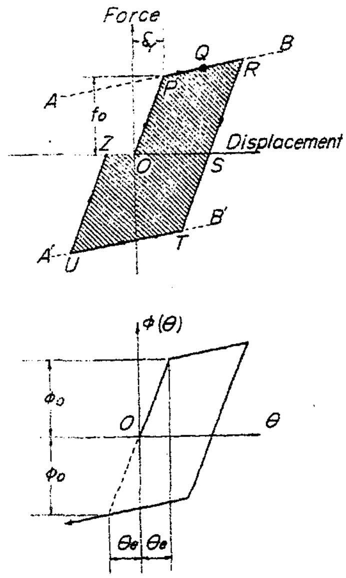

Fig. 2 Bi-linear restitutive characteristic.

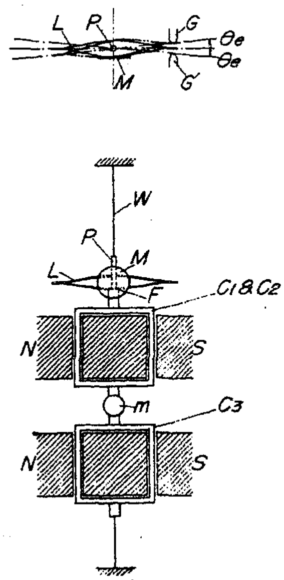

Fig. 3 Vibrator of the type RAC-III analyzer and the structure of its sliding mirror.

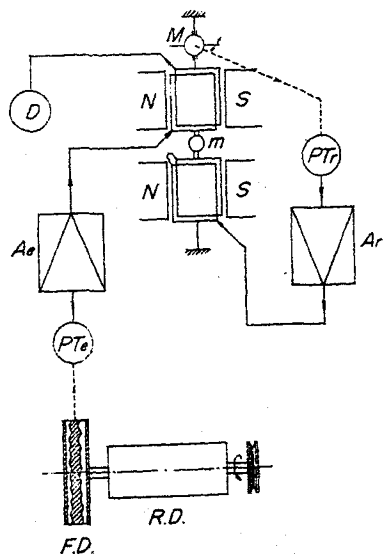

Fig. 4 Block diagram of the type RAC-III analyzer.

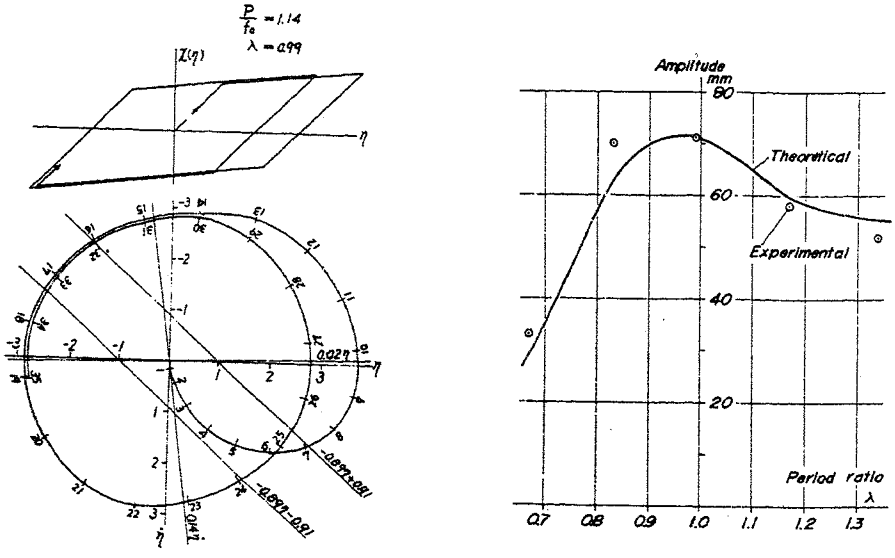

Fig. 6a, 6b Result of calibration of the type RAC-III analyzer by a stationary harmonic input.

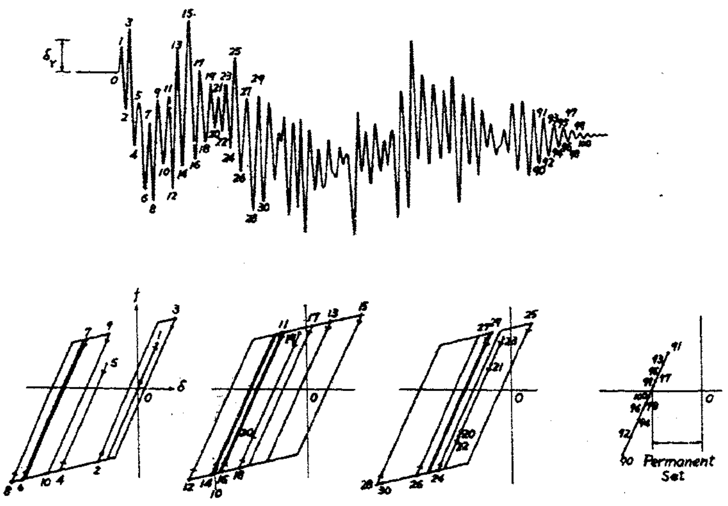

Fig. 7 An example of the response record, El Centro, Calif. earthquake, Dec. 30, 1934. Yield Excursions.

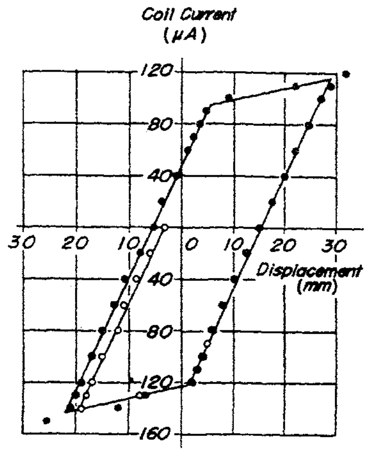

Fig. 5 Result of the statical test of the restitutive characteristic of the type RAC-III vibrator.

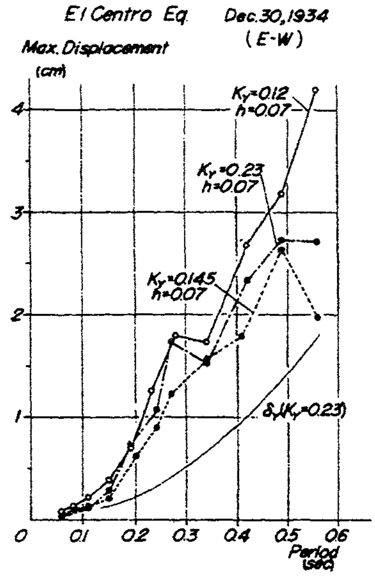

Fig. 8 Hysteresis response spectrum. El Centro, Calif. Earthquake of 1934.

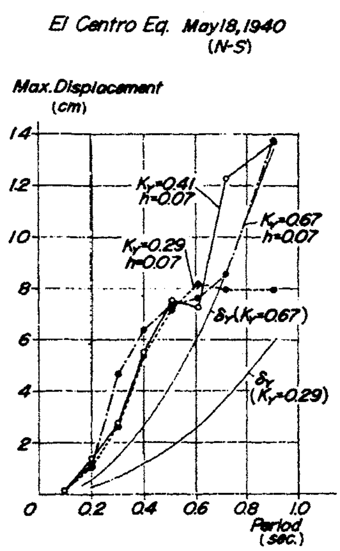

Fig. 9 Do. El Centro Calif. Earthquake of 1940.

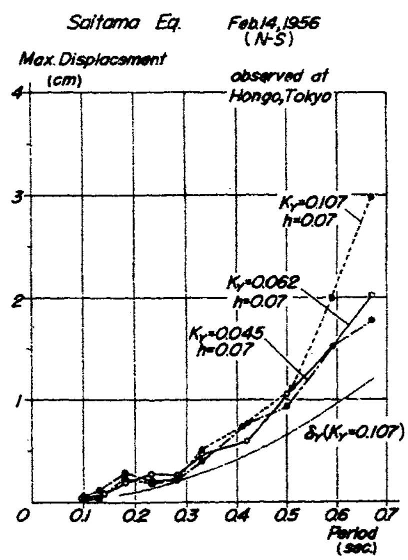

Fig. 10 Do. Saitama Earthquake, Japan, of Feb. 14, 1956.

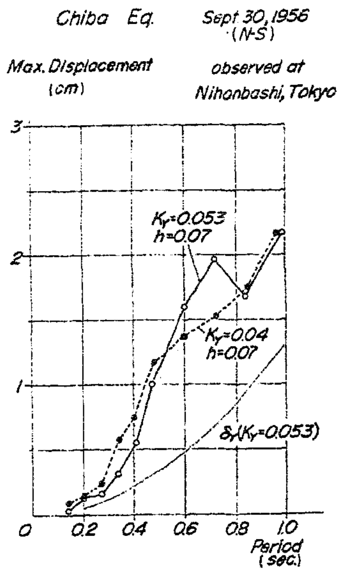

Fig. 11 Do. Chibaken Earthquake, Japan, of Sept. 30. 1956.

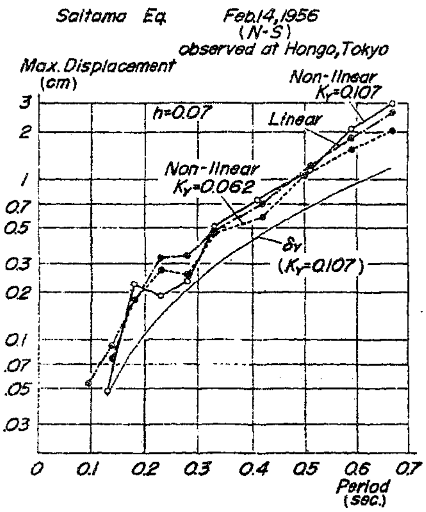

Fig. 12 Comparison of responses of linear and non-linear systems.

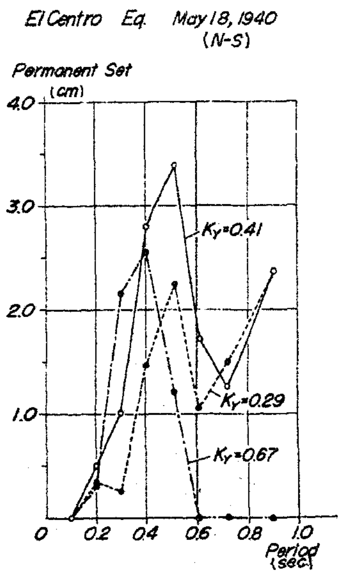

Fig. 13 Permanent set spectrum. El Centro, Calif. Earthquake of 1940.

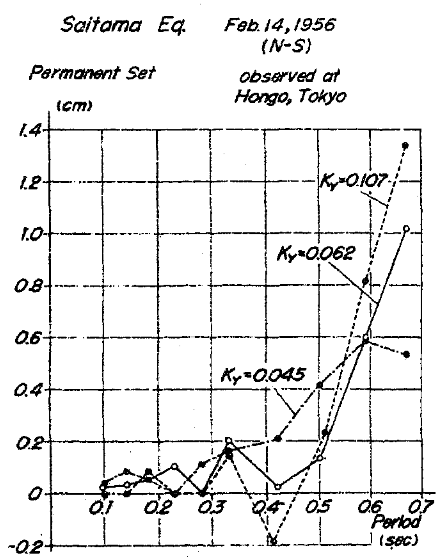

Fig. 14 Do. Saitama Earthquake, Japan, of 1956.

APPENDIX Non-linear Characteristics of Building.

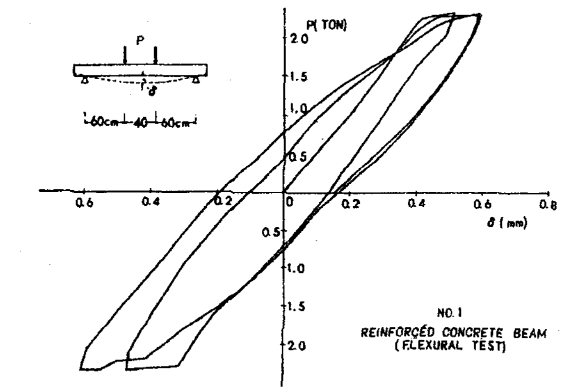

No. 1 REINFORCED CONCRETE BEAM (FLEXURAL TEST)
Reference: S. Fujiwara, "Study on the Reinforced Concrete Beams Subjected to Alternating Load", Graduation Thesis, Dept. of Architecture, Univ. of Tokyo, 1951

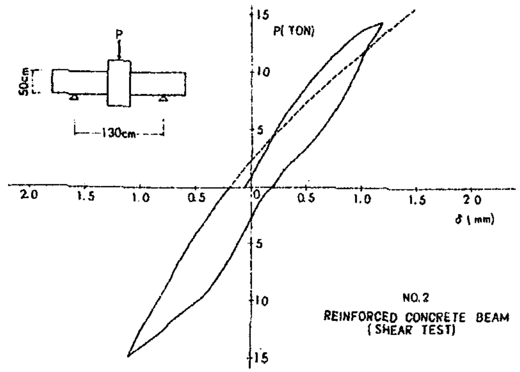

No. 2 REINFORCED CONCRETE BEAM (SHEAR TEST)
Reference: T. Suzuki, "Experimental Study on the Shear Failure of Reinforced Concrete Beams", Graduation Thesis, Dept. of Architecture, Univ. of Tokyo, 1953.

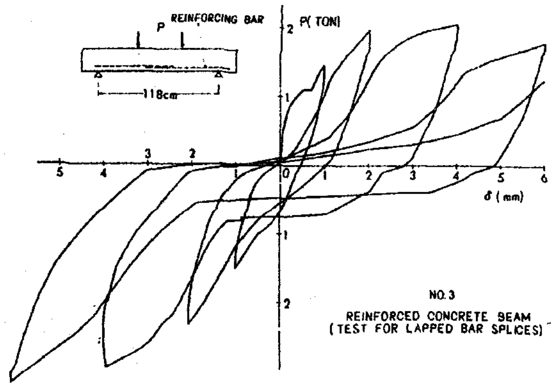

No. 3 REINFORCED CONCRETE BEAM (TEST FOR LAPPED BAR SPLICES) Reference: H. Umemura and T. Takeda, "Experimental Study on the Reinforced Concrete Beams with Lapped Bar Splices" (to be published).

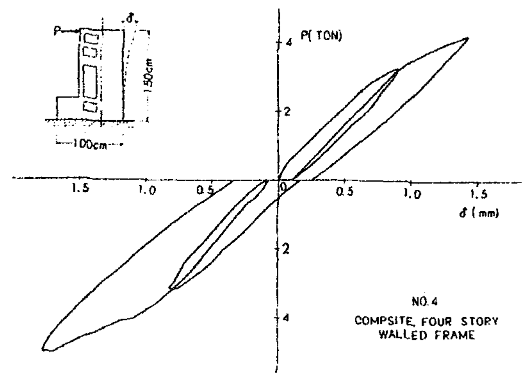

No. 4 COMPOSITE, FOUR STORY WALLED FRAME
Reference: K. Muto, "Experimental Study on the Seismic Wall of the Tokyo Metropolitan Office Building", Report of Muto Laboratory, 1954.

DISCUSSION

G. W. Housner, California Institute of Technology, U. S. A.:

Were experiments carried out on different characteristics of the four-displacement diagrams?

R. Takahashi:

The slope ratio of the bi-linear characteristics in the force-displacement plane can be changed by changing the amplification of the amplifier Ar. We didn't however change this ratio, and kept the characteristics constant all through analyses.